Immunobiology 222 (2017) 518–528

Contents lists available at ScienceDirect

Immunobiology

journal homepage: www.elsevier.com/locate/imbio

Expression and characterization of recombinant chicken mannose binding lectin

Weidong Zhang[a], Martin van Eijk[a], Hongbo Guo[b], Albert van Dijk[a], Onno B. Bleijerveld[c], M. Hélène Verheije[d], Guanbo Wang[e,1], Henk P. Haagsman[a], Edwin J.A. Veldhuizen[a,*]

[a] Division of Molecular Host Defense, Department of Infectious Diseases and Immunology, Faculty of Veterinary Medicine, Utrecht University, The Netherlands
[b] Division of Virology, Department of Infectious Diseases and Immunology, Faculty of Veterinary Medicine, Utrecht University, The Netherlands
[c] Mass Spectrometry/Proteomics Facility, The Netherlands Cancer Institute, Amsterdam, The Netherlands
[d] Division of Pathology, Department of Pathobiology, Faculty of Veterinary Medicine, Utrecht University, The Netherlands
[e] Biomolecular Mass Spectrometry and Proteomics, Bijvoet Center for Biomolecular Research and Utrecht Institute for Pharmaceutical Sciences, Utrecht University & Netherlands Proteomics Center, Utrecht, The Netherlands

ARTICLE INFO

Article history:
Received 19 August 2016
Received in revised form 24 October 2016
Accepted 27 October 2016
Available online 29 October 2016

Keywords:
Collectin
Innate immunity
Chicken
C-type lectin

ABSTRACT

Mannose binding lectin (MBL) is a serum collagenous C-type lectin that plays an important role in the innate immune protection against pathogens. Previously, human and mouse studies have demonstrated that MBL binds a broad range of pathogens that results in their neutralization through agglutination, enhanced phagocytosis, and/or complement activation via the lectin pathway. The role of MBL in chicken is not well understood although the MBL concentration in serum seems to correlate with protection against infections. To investigate the role of MBL in chicken further, recombinant chicken MBL (RcMBL) was produced in HeLa R19 cells and purified using mannan affinity chromatography followed by gel filtration. RcMBL was shown to be structurally and functionally similar to native chicken MBL (NcMBL) isolated from serum. RcMBL is expressed as an oligomeric protein (mixture of trimers and oligomerized trimers) with a monomeric mass of 26 kDa as determined by mass spectrometry, corresponding to the predicted mass. Glycan array analysis indicated that RcMBL bound most strongly to high-mannose glycans but also glycans with terminal fucose and GlcNac residues. The biological activity of RcMBL was demonstrated via its capacity to agglutinate *Salmonella* Typhimurium and to inhibit the hemagglutination activity of influenza A virus. The production of a structurally well-characterized and functionally active RcMBL will facilitate detailed studies into the protective role of MBL in innate defense against pathogens in chicken and other avian species.

1. Introduction

Mannose binding lectin (MBL) is a serum collectin (collagenous C-type lectin), which plays an important role in the innate immune response. Like all members of the collectin family, MBL binds and recognizes a wide range of pathogens, including fungi, bacteria, viruses and parasites, leading to agglutination and neutralization of these microorganisms. In addition, the attachment of MBL to the microbial surface induces the innate immune responses, such as enhanced phagocytosis by macrophages. A third, probably best known function of MBL is that it can activate the complement system via the lectin pathway. MBL binding to pathogens activates MBL-associated serine protease (MASP)-1 and MASP-2, of which the latter cleaves complement factors C4 and C2 to generate a C3 convertase, C4bC2a, aiding in clearance of infection (Dommett et al., 2006; Ikeda et al., 1987; Ip et al., 2009; Thiel et al., 1997). Many studies have underlined the importance of MBL in human and other mammalian species, often showing correlation between low levels of serum hMBL (or hMBL-deficiency) are with susceptibility to bacterial and viral infections (Davies et al., 2004; Hibberd et al., 1999; Ling et al., 2012; Shi et al., 2004). However, there are some conflicting reports as well describing detrimental effects of (higher levels of) MBL, indicating that MBL function in vivo is very complex, as summarized nicely in a recent meta-analysis on cor-

* Corresponding author at: Department of Infectious Diseases and Immunology, Division of Molecular Host Defence, Faculty of Veterinary Medicine, Utrecht University, P.O. Box 80.165, 3508TD, Utrecht, The Netherlands.
E-mail address: E.J.A.Veldhuizen@uu.nl (E.J.A. Veldhuizen).
[1] Current address: School of Chemistry and Materials Science, Nanjing Normal University, China.

http://dx.doi.org/10.1016/j.imbio.2016.10.019

relation between MBL levels and disease susceptibility in human (Heitzeneder et al., 2012).

MBL is synthesized in the liver and is predominantly present in blood serum as multimeric proteins (Sheriff et al., 1994; Turner, 1996). The polypeptide domain organization of MBL is shared by all members of the collectin family and is characterized by a short N-terminal cysteine-rich region, a collagen-like region containing Gly-Xaa-Yaa repeats, and an α-helical coiled-coil neck region followed by a carbohydrate recognition domain (CRD, or lectin domain). The neck region initiates trimerization of three polypeptides to form the functional subunit of MBL which is stabilized by the formation of the collagen triple helix and a disulfide bond between cysteine residues at the N-terminal domain of MBL (reviewed by (Petersen et al., 2001)). Trimerization of MBL not only facilitates the formation of the collagen triple helix but also generates a cluster of three adjacent CRDs that makes MBL, like all collectins, a "pattern recognition molecule", having the ability to interact with specific pathogen-associated molecular patterns (PAMPs). Further oligomerization of trimers is established through N-terminal linkage of MBL trimers. Human MBL is assembled into various degrees of multimerization, ranging from dimers to hexamers of trimeric subunits that resemble a "bouquet of tulips", as visualized by electron microscopy (Jensenius et al., 2009; Lu et al., 1990).

Previously, MBL has been isolated from chicken serum and was characterized as a complex of oligomers consisting of 3–6 trimeric subunits (Laursen et al., 1995). The average chicken MBL (cMBL) concentration in serum is approximately 6 μg/ml but there is a high concentration range among chicken (between 0.4–37.8 μg/ml), possibly caused by polymorphisms in the promotor region of cMBL (Kjaerup et al., 2013). However, based on studies with 308 chickens, representing 14 different chicken lines, no cMBL-deficiency has been found in any of these different breeds (Laursen et al., 1998b). The deduced amino acid sequence of cMBL shares approximately 40% similarity with mammalian MBLs, in which especially the collagen-like domain and the neck region are highly conserved (Laursen et al., 1998a). Like for all MBLs, serum derived cMBL binds carbohydrates via its CRD in a Ca^{2+}-dependent manner and the sugar binding selectivity of cMBL is similar to that of hMBL (Laursen et al., 1995).

Only a few studies have shed light on the functional importance of MBL in chicken. Most *in vivo* studies have been performed with two chicken inbred lines with relatively high (L10H) or low (L10L) serum concentrations of cMBL as compared to outbred lines (Juul-Madsen et al., 2007). The concentration of cMBL seems to correlate inversely with bacterial and viral infections in these two inbred lines. In an *E. coli* challenge experiment, L10L chicken showed significantly reduced gain in body weight upon infection than L10H chicken (Norup et al., 2009). Furthermore it was shown that upon infectious bronchitis virus infection, cMBL acted as an acute phase protein, inhibited viral propagation in the trachea, possibly by activating the complement system, as cMBL was shown to be able to deposit human C4b on the cMBL/MASP complex (Juul-Madsen et al., 2007).

Detailed studies, aimed to investigate the structure and function of native cMBL (NcMBL) *in vitro,* have been complicated by difficulties in obtaining high yields and consistent batches of purified NcMBL. For human studies, a recombinant version of hMBL was successfully produced using mammalian cells, such as Chinese Hamster Ovary (CHO) cells and Human Embryonic Kidney (HEK) 293 cells, resulting in high yields of recombinant human MBL (RhMBL) with structural and functional properties similar to plasma derived hMBL (Ahn et al., 2013; Ohtani et al., 1999; Vorup-Jensen et al., 2001). In our study, this approach was adapted and further modified to produce recombinant chicken MBL (RcMBL) using Human Cervical adenocarcinoma (HeLa) R19 cells. In this paper we describe the production and characterization of RcMBL that exhibits structural and functional characteristics similar to that of NcMBL. The availability of well-characterized and fully functional RcMBL will be an important tool to enable further studies into especially molecular MBL-pathogen interactions in aid to identify MBLs role in infections in chicken and other avian species.

2. Materials and methods

2.1. RNA isolation and cloning of MBL cDNA

Total RNA was obtained from chicken liver tissue (Ross 308) using the High Pure RNA Tissue Kit (Roche, Germany) and digested with DNase I (Roche) to eliminate genomic contamination. The first – strand cDNA was synthesized using the iScript cDNA synthesis kit (BIO – RAD, USA). The coding sequence (CDS) of cMBL, without the signal peptide's sequence (GenBank Accession No. AF231714) was obtained by polymerase chain reaction (PCR) using gene specific primers. Forward primer: 5′ – GAG CTA GCG TTA CTT ACC ACA GAT AAA CCT G –3′, and reverse primer: 5′ – GAT TAA TTA ATC ACA ATT CAC AAA TAA TGA AG –3′. PCR amplification was performed at 95 °C for 5 min, followed by 40 cycles at 95 °C for 30 s, 53 °C for 30 s, 72 °C for 150s, and a final extension at 72 °C for 7 min. The PCR product was purified using the QIAEX II Gel Extraction Kit (Qiagen, Germany) and ligated into the pJET cloning vector (Thermo Scientific, USA), afterwards transformed into DH5α competent cells (Invitrogen, USA). The positive clones were selected and sequenced. The amplified DNA fragment was digested with *NheI* and *PacI* and sub-cloned into the expression vector pFRT (Thermo Scientific) which was previously cut with the same restriction enzymes. The resulting construct, pFRT – cMBL was verified by sequencing analysis.

2.2. Recombinant expression of cMBL using Hela cells

HeLa R19 cells, a gift from Dr. Wentao Li (Utrecht University, The Netherlands), were used to produce RcMBL. The cells were maintained in a humidified 37 °C incubator with 5% CO_2, and cultured in Dulbecco's Modified Eagle Medium (DMEM, Gibco, United Kingdom) supplemented with 10% Fetal Bovine Serum (FBS) (Bodinco BV, The Netherlands), penicillin (100 units/ml) and streptomycin (100 μg/ml). The pFRT expression vector containing the cMBL encoding sequence was transfected into 80% confluent Hela R19 cells using polyethyleneimine (PEI) (Polysciences, USA) in a 1:5 ratio (μg DNA: μg PEI). At 12 h post transfection, the transfection mixture was replaced by 293 SFM II expression medium (Gibco), supplemented with GlutaMax (10 ml/liter, Gibco), primatone (3 g/l, Sigma – Aldrich, USA), D-glucose (2 g/l, Sigma – Aldrich), sodium bicarbonate (3.7 g/l, Merck, Germany), DMSO (15 ml/l, Sigma – Aldrich), penicillin (100 units/ml) and streptomycin (100 μg/ml). The expression medium was harvested at 5 days post transfection (de Vries et al., 2010; Longo et al., 2013).

2.3. Purification of RcMBL

RcMBL was purified from the HeLa R19 expression medium using mannan affinity chromatography. The medium was calcified to a final concentration of 5 mM $CaCl_2$ followed by addition of mannan agarose beads (4 ml bed volume of beads/l of medium, Sigma – Aldrich) and incubated while shaking overnight at 4 °C. The beads were collected and washed extensively with TBS/Ca^{2+} buffer (10 mM Tris – HCl pH = 7.4, 150 mM NaCl, 5 mM $CaCl_2$) to remove all unspecific bound proteins.

Mannan bound RcMBL was eluted with TBS/EDTA buffer (10 mM Tris – HCl pH = 7.4, 150 mM NaCl, 5 mM EDTA), passed through a 0.22 μm filter and concentrated to approximately 1.5 ml using

Amicon Ultra – 15 centrifugal filters (Merck Millipore, Germany) with a cut-off of 10 kDa. Next, the concentrated RcMBL was subjected to gel filtration chromatography to separate the various oligomeric forms of RcMBL using an ÄKTA purifier10 system (GE Healthcare Bio Sciences, Sweden), that was equipped with a Hiload 16/60 Superdex 200 PREP GRADE column and equilibrated in TBS buffer (10 mM Tris – HCl pH = 7.4, 150 mM NaCl). Fractions from each eluted peak were analyzed by non-reducing or reducing SDS – PAGE. Pooled fractions were concentrated by Amicon Ultra – 15 centrifugation and stored in aliquots at −20 °C.

2.4. SDS-PAGE and western blotting of RcMBL

The concentration of purified RcMBL was determined using a BCA Protein Assay Kit (Thermo Scientific). Protein samples were separated on Mini-Protean TGX 4–15% precast gels (Bio-Rad, USA) under reducing or non-reducing conditions, and subsequently visualized by EZBlue gel staining reagent (Sigma – Aldrich) or transferred onto 0.2 μm Nitrocellulose membranes (Bio – Rad) for Western blotting analysis. Immunodetection of RcMBL was performed using a mouse monoclonal antibody against cMBL (6B11, HYB 182 – 01 – 02, Thermo Scientific) according to the manufacturer's instructions. The secondary antibody used was a goat anti – mouse IgG – Peroxidase (Sigma – Aldrich).

2.5. Sequence alignment of the CRD of cMBL with mammalian MBLs and structural modelling of cMBL

Chicken and mammalian MBLs and human SP-D (hSP-D) sequences were obtained from the National Center for Biotechnology Information with the following Genbank accession codes: human SP-D (hSP-D; L05483.1), chicken MBL (cMBL; AF231714.1), human MBL (hMBL; CAB56124.1), canine MBL-C (caMBLC; XP_536402.2), monkey MBL-A and −C (moMBL-A; XP_001096399 and moMBL-C; NP_001099005.1), rat MBL (rMBL; NM_012599.2), mouse MBL (mMBL; NM_010775.2), bovine MBL (bMBL; AAI09675.1), porcine MBL-A and −C (pMBLA; NP_001007195.1 and pMBLC; NP_999290.1). The structural modelling of the neck region and the CRD of cMBL was predicted using iTASSER software as described previously (Yang et al., 2015).

2.6. Liquid chromatography-tandem mass spectrometry (LC–MS/MS) of RcMBL

RcMBL (200 μg/ml, stored in TBS buffer) was diluted with XT sample buffer (Bio-Rad) and proteins were subsequently separated on a precast 12% Bis-Tris gel (Bio-Rad) under reducing conditions. After staining of the SDS-PAGE gel with GelCode Blue stain (Pierce, USA), the RcMBL protein band was excised, proteins in the gel plug were reduced with DTT (1 h at 60° C) and subsequently alkylated using chloroacetamide (30 min at RT in the dark). In-gel digestion with 3 ng/μl trypsin (Gold, Mass Spectrometry Grade, Promega) in 50 mM ammonium bicarbonate (pH = 8.5) was performed overnight at 37 °C. After digestion, the RcMBL-derived peptides were extracted with acetonitrile and dried in a speed vacuum centrifuge. Prior to mass spectrometry analysis, the peptides were reconstituted in 10% formic acid.

Peptides were separated using the Proxeon nLC 1000 system (Thermo Scientific, Bremen) fitted with a trapping column (ReproSil-Pur 120 C18-AQ 3 μm (Dr. Maisch GmbH, Ammerbuch, Germany); 100 μm x 30 mm) and an analytical column (ReproSil-Pur 120 C18-AQ 2.4 μm (Dr. Maisch GmbH); 75 μm x 500 mm), both packed in-house. The outlet of the analytical column was coupled directly to a Thermo Orbitrap Fusion hybrid mass spectrometer (Q-OT-qIT, Thermo Scientific) using the Proxeon nanoflex source. Nanospray was achieved using a distally coated fused silica tip emitter (generated in-house, o.d. 375 μm, i.d. 20 μm) operated at 2.1 kV. Solvent A was 0.1% formic acid/water and solvent B was 0.1% formic acid/ACN. An aliquot (25%) of the in-gel digest was eluted from the analytical column at a constant flow rate of 250 μl/min in a 35-min gradient, containing a linear increase from 7% to 25% solvent B, followed by wash at 80% solvent B. Survey scans of peptide precursors from m/z 375–1500 were performed at 120 K resolution with a 4×10^5 ion count target. Tandem MS was performed by quadrupole isolation at 1.6 Th, followed by HCD fragmentation with normalized collision energy of 33 and ion trap MS2 fragment detection. The MS2 ion count target was set to 10^4 and the max injection time was set to 50 ms. Only precursors with charge state 2–6 were sampled for MS2. Monoisotopic precursor selection was turned on; the dynamic exclusion duration was set to 30 s with a 10 ppm tolerance around the selected precursor and its isotopes. The instrument was run in top speed mode with 3 s cycles.

Raw data files were processed using Proteome Discoverer (version 1.4.1.14, Thermo Fisher Scientific). MS2 spectra were searched against the Uniprot chicken database (Uniprot Gallus Gallus, release 20110418, 15344 sequences) using Mascot (version 2.4.1, Matrix Science, UK). Carbamidomethylation of cysteines was set as fixed modification and oxidation of methionine was set as a variable modification. Trypsin was specified as protease and up to two miscleavages were allowed. Data filtering was performed using percolator, resulting in 1% false discovery rate (FDR) at peptide level, and peptide ion score >20.

2.7. Native mass spectrometry

The native mass spectrometry measurements used to determine protein oligomeric states and obtain total mass were conducted with a modified Q-ToF (Waters, UK) mass spectrometer adjusted for enhanced performance in tandem MS (van den Heuvel et al., 2006). RcMBL (stored in TBS buffer) were substituted with a 150 mM ammonium acetate solution through sequential concentration and dilution steps at 4 °C using Amicon Ultra – 15 centrifugal filter (Merck Millipore) with a cut-off of 10 kDa. Samples were sprayed using a standard static nanospray source. Tandem MS analysis was conducted by mass-selection of sub-population of ions using the quadrupole mass analyzer followed by dissociation of precursor ions induced by their collision with xenon atoms. Data were analyzed with MassLynx (Waters, UK) and Origin Pro (Origin Lab, USA) software.

2.8. Glycan array

Glycan binding specificity of RcMBL was determined using the version 5.3 glycan array of the Consortium for Functional Glycomics (CFG). This array consists of 601 glycans, structures and their corresponding CFG numbers are available at the website of the CFG (http://www.functionalglycomics.org/). Glycan binding was performed essentially as described (Blixt et al., 2004). In brief, RcMBL (2 or 20 μg/ml) was applied to the Glycan array slides in Binding buffer (150 mM NaCl, 2 mM CaCl2, 2 mM MgCl2, 0.05% Tween-20, 20 mM Tris-HCl, pH = 7.4), and subsequently incubated with Anti-chicken MBL antibody (HYB 182-01-02, Thermo Scientific) in Binding buffer (1: 2000 dilution) for 60 min at RT. Microarray slides were washed by successive rinses in TPBS buffer (PBS with 0.05% Tween-20), and overlaid with an Alexafluor 488 labeled goat anti-mouse-IgG secondary antibodies in phosphate buffered saline (PBS) containing 0.5% Tween-20. After repeated washes with TPBS, PBS and deionized water the slides were immediately subjected to imaging. Fluorescent signal intensity was measured using IMAGENE image analysis software (BioDiscovery, EI Segundo, CA), mean intensity minus mean background was calculated using Microsoft EXCEL software. For each glycan, the mean signal intensity is calculated

from 6 replicates spots. The highest and the lowest signals of the 6 replicates were removed and the remaining 4 replicates were used to calculate the mean signal, standard deviation.

2.9. Salmonella typhimurium agglutination assay

RcMBL-induced bacterial agglutination was assessed by confocal microscopy. *Salmonella* Typhimurium (DT104) was grown in Mueller Hinton Broth (MHB, Sigma – Aldrich) at 37 °C until midlog – phase, afterwards the bacteria were spun down and resuspended in TBS buffer to a density of 1×10^8 CFU/ml. A hundred μl of bacterial suspension was incubated with various concentrations of RcMBL in the presence of 5 mM $CaCl_2$ for 1 h at 37 °C. Next, the live/dead staining was performed on the bacteria using the BacLight bacterial viability kit (Invitrogen, USA) with the permeant fluorescent probe SYTO 9 and the impermeant fluorescent probe propidium iodide (PI) according to the manufacturer's protocol, in which SYTO 9 and PI stain live (green) and dead (red) cells, respectively. The mixture was added on top of a 35 mm FluoroDish (WPI, USA) immediately followed by visual analysis with a Leica SPE-II-DMI4000 confocal microscope at the Center for Cell Imaging (CCI), Utrecht University, using 100 × /1.4 – numerical aperture objective. Live and dead staining were visualized at 405 nm and 635 nm, respectively. Representative pictures were obtained after 20 times screen.

2.10. Hemagglutination inhibition (HAI) assay

The IAV strains used in this study were a human isolate A/Philippines/82(H3N2) (Phil82) and A/PuertoRico/8/34 (H1N1) (PR-8) that lacks high-mannose oligosaccharides on the globular domain of its hemagglutinin (HA). The IAV strains were grown in chorioallantoic fluid of 10-day-old chicken eggs and purified on a discontinuous sucrose gradient centrifuge. Virus stocks were stored at −80 °C after dialysis against PBS++ (PBS with 1 mM $CaCl_2$ and 0.5 mM $MgCl_2$). The hemagglutination titer of each virus was determined by titration of virus sample in PBS++ with thoroughly washed human type O, Rh (−) red blood cells (RBC). The HI test was performed by serially diluting RcMBL (25 μl) in round bottom 96 – well plates using PBS++ or PBS++ containing 5 mM EDTA (negative control) as diluents. After adding 25 μl of IAV (4 hemagglutination units) in each well, the IAV/RcMBL mixture was incubated for 30 min at 37 °C. Fifty μl RBC (1% suspension in PBS++) was added to each well and the plates were incubated for 2 h at RT. The inhibition was detected by the formation of erythrocyte pellets as described previously (van Eijk et al., 2011).

3. Results

3.1. Purification and characterization of RcMBL

RcMBL was successfully expressed in Hela R19 cells and purified from the expression supernatant by affinity chromatography using mannan agarose beads. The average protein yield was 1.5 – 2.0 mg from 1 l of expression culture. The eluted protein was analyzed by SDS – PAGE and Western blotting. NcMBL, partially purified from chicken serum, was used for structural comparison analysis. Both RcMBL and NcMBL showed a band of 33 kDa after Western blotting under reducing conditions (Fig. 1). Mannan-purified RcMBL was subjected to size-exclusion chromatography and separated into two main peaks (Fig. 2A). Pooled fractions from each peak were analyzed by SDS – PAGE and Western blotting. Under non-reducing conditions the results showed that peak 1 consisted of higher order oligomeric structures of RcMBL with molecular weights from 120 to 250 kDa and above, while peak 2 contained mainly trimeric structures ranging from 33 to 70 kDa (Fig. 2B). Under reducing conditions

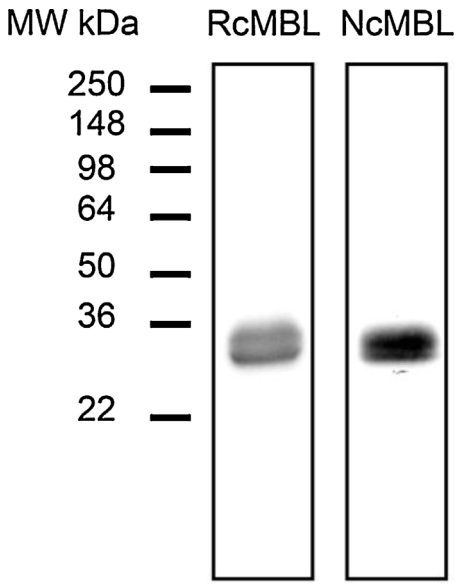

Fig. 1. Western blotting analysis of RcMBL and NcMBL.
Ten μg mannan-purified RcMBL and serum-derived NcMBL were analyzed using SDS-PAGE on a 4–15% pre-casting gradient gel under reducing conditions. Visualization of cMBL was done using an anti-chicken MBL monoclonal antibody (primary) and a goat anti-mouse IgG antibody (secondary).

the results showed that both peaks migrated as a single band of 33 kDa (Fig. 2B).

3.2. Alignment of cMBL with mammalian MBLs and structural modelling

The cMBL sequence (Laursen et al., 1998a) reveals that its CRD contains all sequence features of a C-type lectin and is highly comparable to MBL from other animal species (Fig. 3A). The two most important structural elements of C-type lectins are the 4 cysteines that stabilize the characteristic double loop structure (Cys159-Cys251, Cys228-Cys242) and the 218-EPN-220, 237-WND-239 motifs that are required for ligand binding through coordination of a calcium ion in the binding pocket of MBL (Veldhuizen et al., 2011). All these features are also present in cMBL which is consistent with the observed Ca^{2+}-dependent binding of glycans by cMBL during purification. The predicted 3 dimensional backbone structure of the neck CRD of cMBL also indicates clearly that cMBL adopts the classical C-type lectin fold, highly similar to the neck-CRD of hMBL and to the neck-CRD of human surfactant protein D (hSP-D) (Fig. 3B–D).

3.3. Mass spectrometry

Native mass spectrometry analysis of RcMBL (peak 2, fraction containing the trimers) using regular buffer (NH_4Ac) resulted in a mass spectrum with a charge-state-resolution insufficient for accurate mass determination (Fig. 4A inset), mainly due to the broadly distributed mass of this heterogeneously glycosylated protein. To improve the separation of signals representing protein ions in adjacent charge states we introduced 20% (mol/mol) triethylammonium acetate (TEAA) into the sample solution which can partially reduce the charge states (Dyachenko et al., 2013). The resulting mass spectrum of RcMBL showed signals representing three distributions of charge states, each of which represented a single species (Fig. 4A, blue trace). A preliminary deconvolution (Wang et al., 2012) revealed that the molecular weights of the second and third species are two times and three times that of the first species, respectively. Accurate mass determination of these

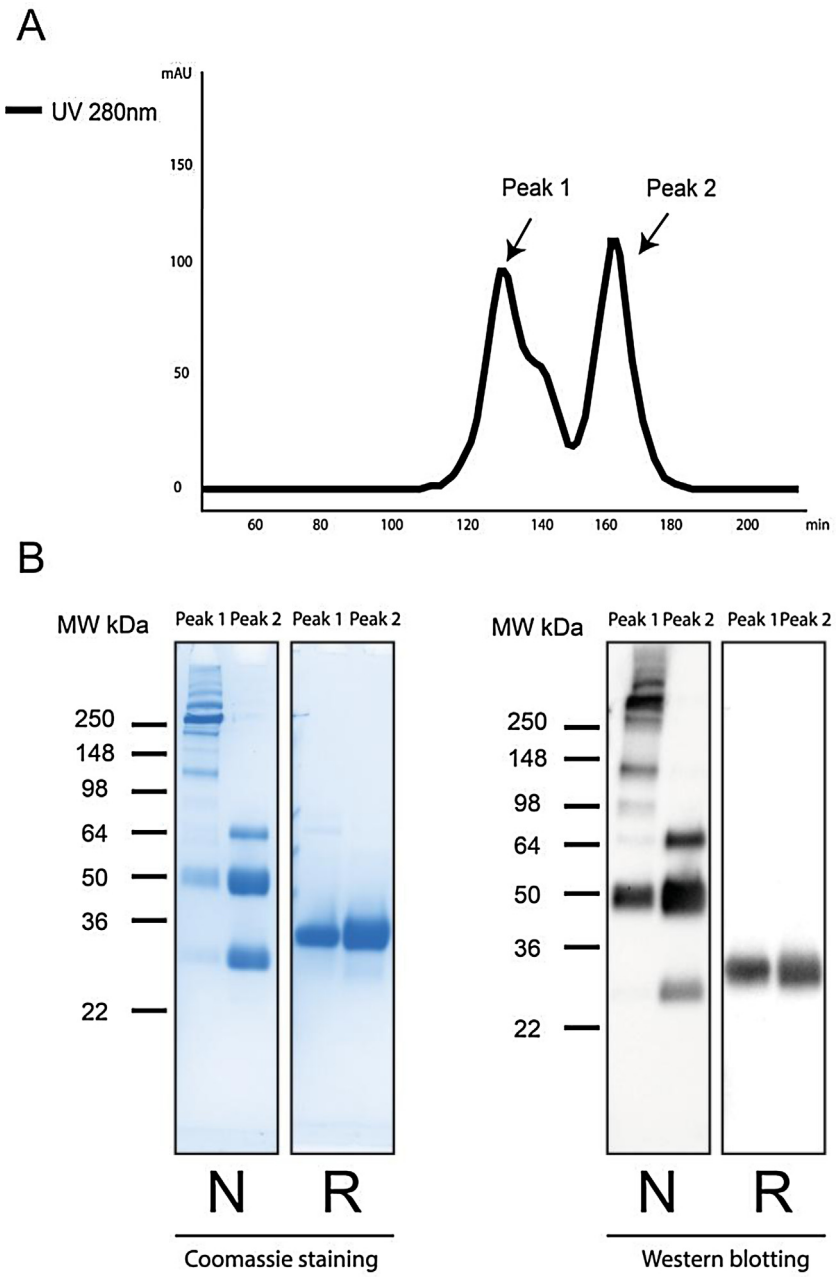

Fig. 2. Purification and size exclusion chromatography of RcMBL.
A) Gel filtration analysis of RcMBL was performed on mannan-affinity purified RcMBL using an ÄKTA purifier10 system with a Hiload 16/60 Superdex 200 PREP GRADE column. The x−axis and ϒ−axis show the elution time (elution speed: 0.5 ml/min) and optical density at 280 nm, respectively. Peak 1 and peak 2 are indicated with arrows. B) SDS – PAGE and Western blotting analysis of pooled fractions of peak 1 and peak 2. Fractions from peak 1 and peak 2 were collected separately and concentrated with Amicon Ultra-15 centrifugal tube (MWCO10). 10 μg of purified RcMBL proteins from peak 1 and peak 2 were analyzed using a 4–15% pre-casting gel under either reducing (R) or non-reducing conditions (N). CMBL was visualized using an anti-chicken MBL monoclonal antibody (primary) and a goat anti-mouse IgG antibody (secondary).

species was performed via tandem MS measurements, where the collision-induced dissociation (CID) employed in the mass analyzer provides the protein analytes with maximal desolvation and specific fragmentation patterns that serve as constraints for accurate charge assignments (Dyachenko et al., 2015). As exemplified in Fig. 4B, under the TEAA-free condition, mass-selection of ions with m/z centered at 4400 (the largest species) and the subsequent CID yielded fragment ions carrying 11–13 positive charges and the corresponding residual species in charge states of 6–8. Accordingly the molecular weight of the three species, as shaded individually in Fig. 4A, were determined as 26.1 ± 0.1 kDa, 52.9 ± 0.3 kDa and 79.2 ± 0.4 kDa, respectively (averages from at least three measurements). These molecular weight values and the relative abundance depicted in Fig. 4A clearly indicate that RcMBL (from the trimer-fraction in Fig. 2A) indeed exists as a trimer of three individual cMBL polypeptides, with minor amounts of monomeric and dimeric species. Intriguingly, based on the adequately resolved signals representing the heterogeneous monomers, the average mass difference between adjacent glycoforms was determined as 0.32 kDa, implying a difference in mass corresponding to 2 hexoses between MBL iso(glyco)forms.

3.4. Glycan array

In order to determine glycan binding specificity of RcMBL, the protein was subjected to glycan array analysis (array version 5.3)

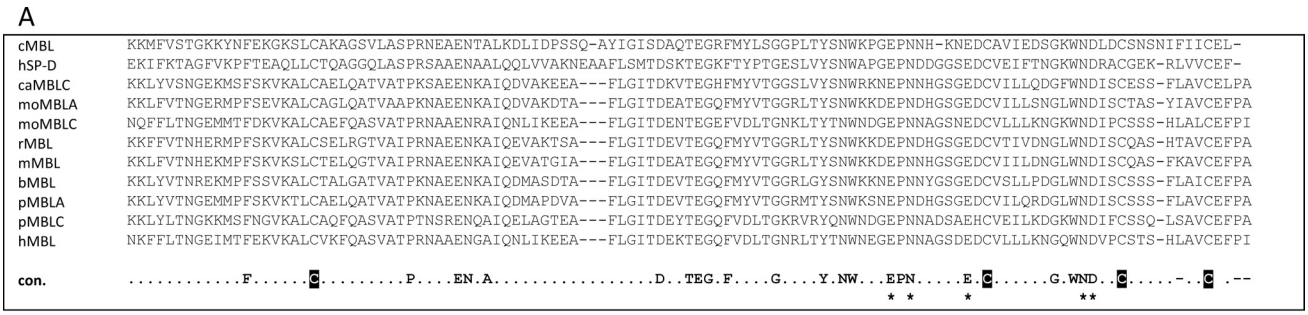

Fig. 3. Comparison of the CRD sequence of MBLs and 3D structure prediction of the neck-CRD region of cMBL.
A) Amino acid sequence alignment of the CRD. Residues in common with the cMBL sequence are indicated with dots and a consensus sequence with residues that are shared by all collectins is also provided 'con'. Asterisks indicate the residues necessary for coordination of Ca^{2+} ions and ligand binding. Four cysteines stabilizing the double loop structure of CRD are indicated with a black shadow. B) The architecture of the cMBL monomer was predicted using the iTasser programme (http://zhanglab.ccmb.med.umich.edu/I-TASSER/). The neck region is depicted in blue, CRD in green and the EPN motif is indicated in red. C) Overlay of the structure of cMBL (green) and hMBL (blue). D) Overlay of the structure of cMBL (green) and hSP-D (red). The pictures are shown in side view (top) and top view (bottom).

in collaboration with the Consortium for Functional Glycomics (as described in Materials and Methods). RcMBL most strongly bound to glycans containing terminal mannose (especially high mannose glycans), fucose or GlcNac residues (Fig. 5). Overall lower binding was observed for glycans containing terminal galactose residues or N-acetylneuraminic acid. Administering a 10-fold higher amount of RcMBL to the array resulted in a slightly different binding order of high binding glycans but very similar overall specificity. A total list of all 601 tested glycans and their binding to (two concentrations of) RcMBL is depicted in Table S1.

3.5. Agglutination

Earlier studies have reported that collectins can directly agglutinate bacteria, fungi and viruses, an important functional property that helps to protect against epithelial infection by these pathogens. Therefore, bacterial agglutination was assessed by incubating mid-log phase suspensions of *Salmonella* Typhimurium with RcMBL (peak 1, 20 and 50 μg/ml), followed by staining with SYTO9 and PI. SYTO9 is a green fluorescent nuclear counterstain which stains both live and dead Gram-negative and Gram-positive bacteria. PI is a red fluorescent nuclear and chromosome counterstain for dead cells only. After adding the dye mixture, samples were inspected for differential nuclear staining using a confocal microscope. RcMBL was able to agglutinate *Salmonella* Typhimurium in a Ca^{2+}-dependent manner, as illustrated by the formation of large aggregates in the presence of calcium that were absent after incubation in the presence of EDTA. The control incubation with calcium ions but in the absence of RcMBL also did not show any agglutination. Direct bacterial killing is not described for mammalian MBL and also RcMBL-induced agglutination did not lead to bacterial death as no obvious PI staining was observed for the RcMBL-treated samples (Fig. 6).

Table 1
Hemagglutination inhibition of IAVs by RcMBL.

RcMBL (μg/ml)		40	20	10	5	2.5	1.25
H3N2 (Phil82)	Calcium	++++	++++	+++	++	+	–
	EDTA	–	–	–	–	–	–
H1N1 (PR-8)	Calcium	++	–	–	–	–	–
	EDTA	–	–	–	–	–	–

RcMBL (peak 1, multimers) was incubated with IAV (4HAU) for 30 min at 37 °C, followed by 2 h incubation with red blood cells (RBC). Hemagglutination inhibition was determined by RcMBL-induced reduction of RBC pellet formation.
'++++' indicates full inhibition of RBC pellet formation.
'+++, ++, +' indicates partial inhibition of RBC pellet formation.
'–' indicates no inhibition of RBC pellet formation.
Data shown is from three independent experiments.

3.6. Hemagglutination inhibition of IAV by RcMBL

The antiviral activity of RcMBL was measured against two subtypes of IAV, H3N2 (PHIL82) and H1N1 (PR-8), using a HAI assay. As shown in Table 1, RcMBL was able to fully inhibit H3N2 IAV induced agglutination of red blood cells at a concentration of 2.5 μg/ml or

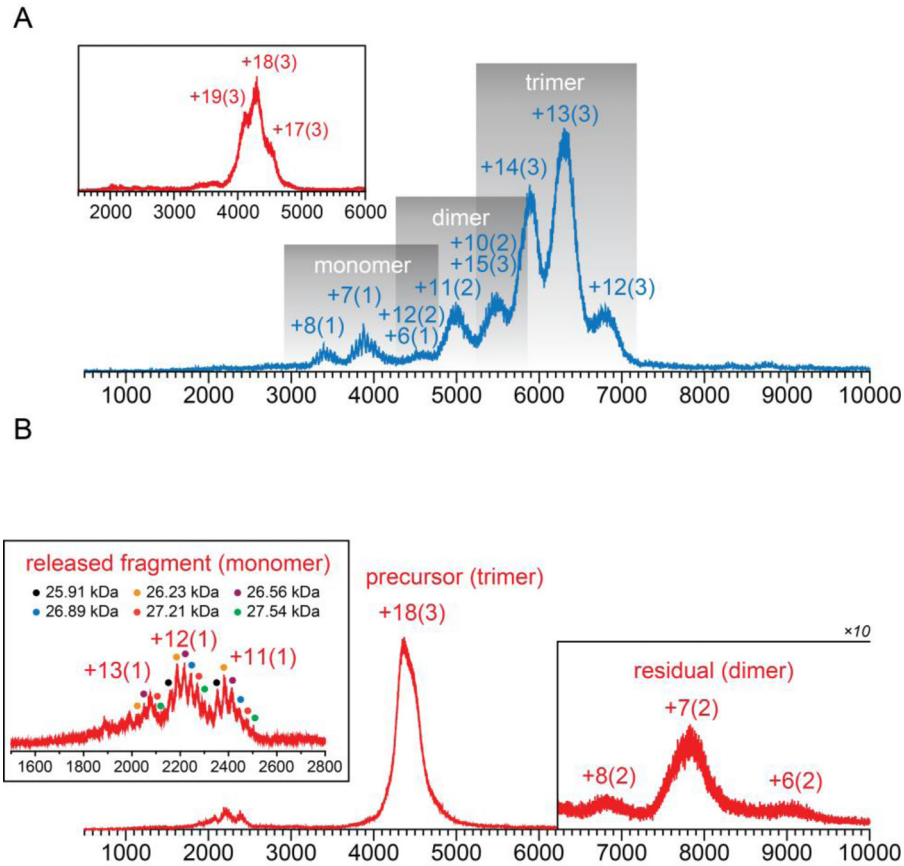

Fig. 4. Oligomerization analysis of RcMBL and molecular weight determination by native mass spectrometry. (For interpretation of the references to colour in this figure legend, the reader is referred to the web version of this article.)
A) Native mass spectra of RcMBL (peak 2, trimers) acquired without (inset, red) and with TEAA (blue). B) A tandem mass spectrum showing the mass-selection of the largest ionic species and its collision-induced dissociation (CID) pattern. The inset shows a close-up view of the released fragment ions. Intensities of the signals representing residual species were magnified by 10 for better visualization. Signal peaks are labeled with the corresponding charge states and oligomeric states (in parentheses).

higher, but was less active against H1N1 IAV as the highest dose tested (40 μg/ml) could only partially inhibit the HA activity of the PR-8 strain. Similar to what was found for RcMBL-induced bacterial agglutination, the HAI activity of RcMBL was also Ca^{2+}-dependent, since all HI activity was inhibited in the presence of EDTA.

4. Discussion

Collectin-mediated innate immune responses play an important role in the first line defense against infections as illustrated by numerous studies in humans and other mammalian species. In avian species, however, not much is known about the specific role of these collagenous C-type lectins, including MBL, the most well-characterized serum collectin. Thus far, only a few studies have provided some insight into the role and function of MBL in avian species and how this contributes to chicken health is still not well addressed. Since the availability of well-characterized purified cMBL is very limited, detailed studies are difficult. Therefore, we aimed to produce a recombinant version of cMBL, and this study describes the high-yield expression of RcMBL by the use of HeLa R19 cells. Our study shows that RcMBL can be produced with structural and functional properties similar to those of chicken serum-derived MBL.

Previous studies have demonstrated that hMBL can also be successfully produced using different mammalian expression systems. HEK 293 cells and CHO cells are the most commonly used cell expression systems, both of which can produce RhMBL that is structurally and functionally similar to native human MBL (NhMBL).

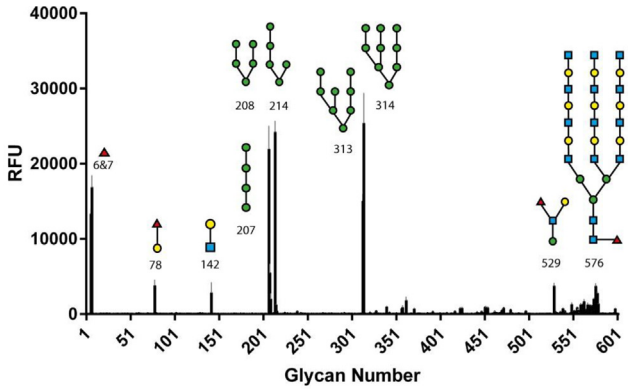

Fig. 5. Glycan array analysis of RcMBL.
The panel shows the mean plus standard deviation of the binding signals for each glycan. The highest binding glycans for RcMBL are depicted schematically in the figure. Glycan numbers indicated on the X-axis corresponds to the structures described in supplementary Table S1. Green cycle: Mannose, yellow cycle: Galactose, red triangle: Fucose, blue square: N-acetyl Glucoseamine.

RhMBL assembles into higher oligomers in those cells, and displays similar carbohydrate binding properties as compared to those of NhMBL. Furthermore, it can inhibit hemagglutination activity of IAV and activate the complement system associated with MASPs (Ahn et al., 2013; Ohtani et al., 1999; Vorup-Jensen et al., 2001).

In our study, HEK 293 and HeLa R19 cells were used for the production of RcMBL. RcMBL was successfully expressed in both

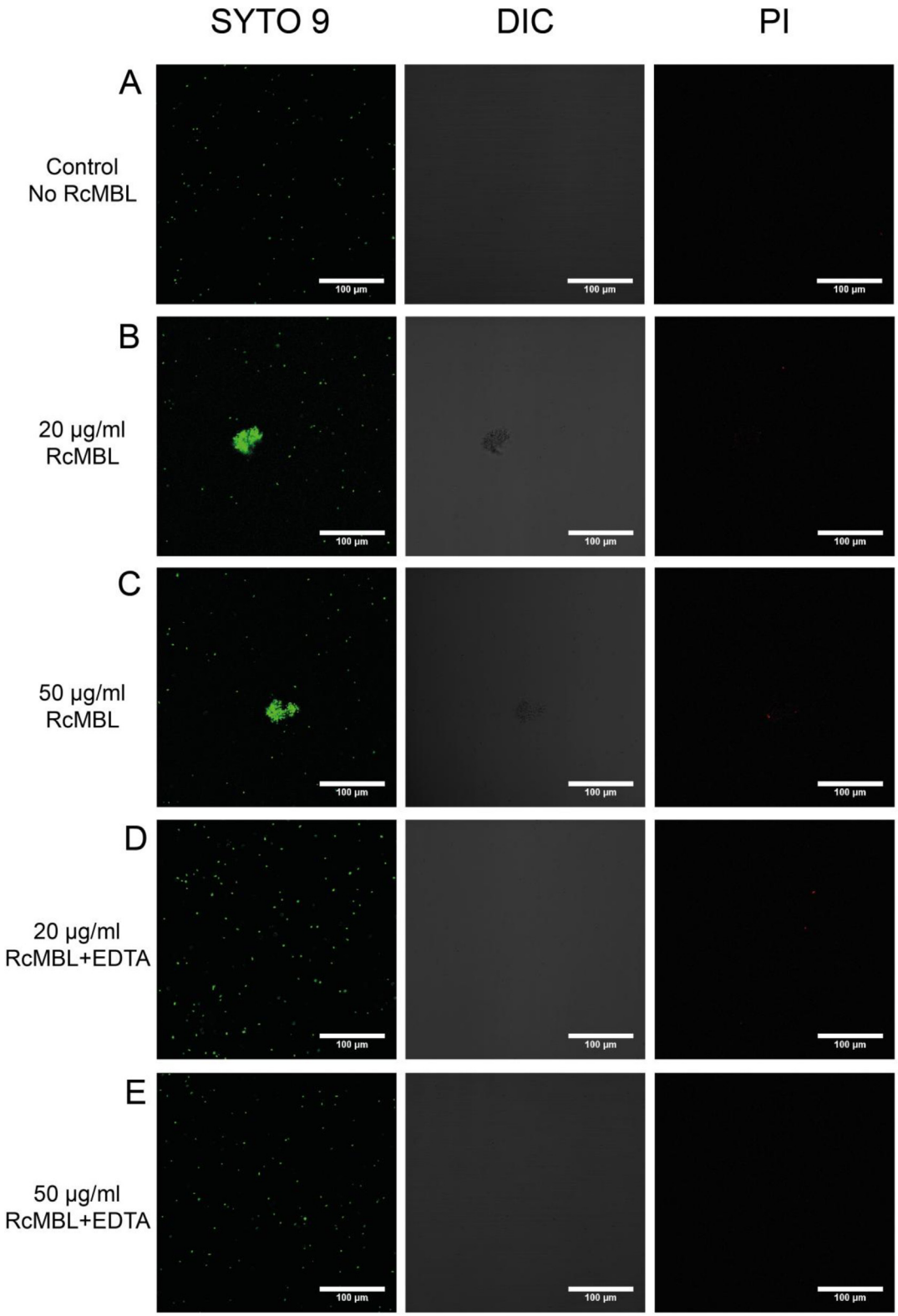

Fig. 6. Ca^{2+}-dependent RcMBL-induced agglutination of *Salmonella* Typhimurium.
RcMBL (peak 1, multimers) was incubated with *Salmonella* Typhimurium (1×10^8 CFU/ml) for 1 h at 37 °C, live/dead staining was performed with fluorescent probe SYTO9 (green) and the impermeant fluorescent probe propidium iodide (red) followed by imaging with confocal microscopy. A) No agglutination was observed with negative control (without RcMBL). B) and C) *Salmonella* Typhimurium agglutination was observed with 20 and 50 μg/ml of RcMBL, respectively, in the presence of 5 mM calcium. D) and E) Agglutination inhibited by EDTA (final concentration of 5 mM) in the presence of 20 or 50 μg/ml of RcMBL, respectively. PI staining indicates the dead cells. Images shown are representative for three separate experiments.

protein expression systems, SDS-PAGE and Western blotting analysis did not reveal major structural differences between both RcMBL preparations. However, the yield of RcMBL expressed in HEK 293 cells was substantially lower and resulted in strong batch-to-batch variations as compared to RcMBL expressed in Hela R19 cells (result not shown). Therefore, RcMBL expressed by HeLa R19 cells was used in the functional and structural characterization studies.

NcMBL is present in serum as an oligomeric protein, heterogeneously assembled into multimeric structures with 2 to 6 trimeric subunits (Kawasaki et al., 1983; Laursen et al., 1995; Mizuno et al., 1981). The oligomerization of our RcMBL was determined by gel filtration and showed that it is assembled as a mixture of trimers and higher order oligomers of trimers, similar to NcMBL (Fig. 2). The majority of oligomers from peak 1 are ranging in mass from 120 to 250 kDa above, while peak 2 mainly contained trimeric protein. Reduced SDS-PAGE revealed that RcMBL was detected as a single band of approximately 33 kDa, which is approximately 7 kDa size bigger than the predicated size based on the cMBL amino acid sequence. Therefore, we also analyzed RcMBL by tandem mass spectrometry and determined that the molecular weight of monomeric RcMBL is approximately 26 kDa, corresponding with the predicted size. This difference is likely due to differences in migration behavior on SDS-PAGE between collagen-containing, more elongated proteins like MBL, as compared to the globular proteins that were used as molecular weight markers in our SDS-PAGE experiments (van Eijk et al., 2002). Western blot analysis of reduced RcMBL and NcMBL showed that both RcMBL and NcMBL migrated as a 33 kDa polypeptide and both stained positive after immunostaining with an anti-cMBL antibody. RcMBL was also identified by LC–MS/MS analysis of protease-treated RcMBL and data showed that more than 70% of the cMBL sequence could be identified in the resulting peptides, indicating that the RcMBL had the correct sequence. Glycosylation of RcMBL was examined by treatment of PNGase and O-glycosidase, where no indications for glycosylation could be observed (result not shown). In addition, there is an absence of putative glycosylation sites based on the cMBL sequence. The presence of two hexoses in some of the MBL preparations, as determined by mass spectrometry, results in differences too small to be determined with a band shift on a gel. Probably, these detected hexoses were ligands, bound by MBL.

MBL, like all collectins, belongs to the C-type lectins and this implies that it only binds glycans via its CRD in a Ca^{2+}-dependent manner. The sugar binding activity of the CRD in C-type lectins is determined by the presence of 5 key conserved amino acid residues (EPN-E-WND) that are coordinated via the presence of a calcium ion to facilitate interactions with mannose-type glycans. These interactions result from the formation of a hydrogen bond network between distinct hydroxyl groups of sugars and amino acid residues of the CRD (Weis et al., 1991, 1992). As previously reported by Laursen (Laursen et al., 1998a), and shown in Fig. 3A, cMBL also contains the EPN-E-WND key residues that are conserved in MBL from all animal species that have been characterized to date (Laursen et al., 1998a). The observed glycan specificity of RcMBL, as determined in this study using a glycan array was indeed typical for a mannose type of C-type lectins. Mainly terminal mannose, N-acetyl glucosamine and fucose residues were required for strong binding to RcMBL. Laursen et al. had previously determined binding specificity of monosaccharides to NcMBL using a competition assay (Laursen et al., 1995). Of the monosaccharides tested ManNac, GlcNac mannose and fucose were capable of inhibiting cMBL binding to mannan. Despite the relative low number of glycans tested, these results correlate well to our results, considering that the glycan array used does not contain terminal ManNac residues. Similarly, glycan binding of MBL of other species also have a mannose type fingerprint (Childs et al., 1990; Haurum et al., 1993) indicating that no major specificity for certain glycan binding seem to exist for avian MBL compared to mammalian MBL. However, more subtle differences could have major functional consequences for recognition of pathogens or host (immune) cells.

The 3-dimensional structure of the neck-CRD domain of cMBL was also predicted by the iTasser programme (Yang et al., 2015). Overlay modelling showed that the neck-CRD fold of cMBL strongly overlaps to that of both hMBL and hSP-D (Fig. 3). Interestingly, the angle between neck and CRD of cMBL seems to resemble more that of hSP-D than hMBL. Any functional consequences for this are only speculative but are worthwhile to investigate. Overall the structure further underlines that the CRD conformation of cMBL fulfills the criteria of being a C-type lectin (the C-type lectin structure has also been reviewed in (Hakansson and Reid, 2000; Veldhuizen et al., 2011)).

The biological activity of RcMBL was investigated by testing its antibacterial and antiviral properties. First, RcMBL was tested for its potency to agglutinate bacteria, using *Salmonella* Typhimurium, a bacterial species known for its wide range host infection, including human and chicken, that causes localized self-limiting gastroenteritis (reviewed in (Calenge et al., 2010; Ohl and Miller, 2001)). The binding of MBL to *Salmonella* is strain-dependent and mainly depends on the degree of glycosylation of the O-antigen, while the 3-dimensional structure of the lipopolysaccharide (LPS) also plays an important role in determining MBL attachment to this microorganism (Devyatyarova-Johnson et al., 2000). In our study, RcMBL was able to agglutinate bacteria into large aggregates in the presence of calcium ions, but this aggregation was no longer observed in the presence of EDTA. This result is in contrast with a previous study that showed that NcMBL was not capable to bind *Salmonella* Typhimurium (Ulrich-Lynge et al., 2015). This difference in outcome might be due to structural differences between individual strains that can influence the interactions with MBL, for instance, the complexity of glycan on the microbial surface, the structure and composition of bacterial endotoxins, and the expression of capsular polysaccharide of bacteria (Neth et al., 2000).

It has been described in several studies that collectins also play an important role in neutralization of viral infections, including MBL (Hartshorn et al., 1997). We also tested RcMBL for its HAI activity against different subtypes of IAV. The *in vitro* interactions between MBL and IAV has been well-documented, including inhibition of viral hemagglutination, blocking of viral neuraminidase activity, opsonization of IAV resulting in increased uptake and activation of neutrophils, neutralization of IAV infectivity, and activation of the complement system to promote lysis of IAV or IAV-infected cells (reviewed in (Ng et al., 2012)). The binding of MBL to IAVs occurs via interactions between the CRD of MBL, and the glycosylated viral spike proteins HA and NA, and depends on the degree and location of N-glycosylations present on the globular head region of HA (Job et al., 2010; Reading et al., 1997). This is illustrated by studies with the PR-8 (H1N1) strain which is highly resistant to binding and neutralization by MBL as well as SP-D, because PR-8 does not carry any glycosylation sites on the head region of its HA (Reading et al., 1997). The presence of mannose-type oligosaccharides on the HA domain of IAV is considered the discriminating factor that determines interactions between MBL and IAVs. This is further illustrated by the ability of MBL to neutralize Phil82 (H3N2) much more efficiently as compared to the mutant strain Phil82BS which lacks the high-mannose glycan moiety overlying the receptor binding site of the parent Phil82 strain (Chang et al., 2010). In our study, we tested the HAI activity of RcMBL against both PR-8 (H1N1) and Phil82 (H3N2) and, as expected, RcMBL exhibits strong HAI activity against H3N2 requiring a relatively low concentration of RcMBL (2.5 μg/ml) for neutralization of this strain. In contrast, the HAI activity of RcMBL on H1N1 is very limited, only the highest concentration tested (40 μg/ml) can partially inhibit the viral-induced agglutination of red blood cells.

The HAI activity of RcMBL against IAV is completely lost in the presence of EDTA, indicating that the interaction between RcMBL and IAV is mediated via the Ca^{2+}-dependent CRD of RcMBL, similar to what was found for hMBL and SP-D. Taken together, these findings underline that the CRD of RcMBL is fully functional in the presence of calcium ions, and that this domain is responsible for the interactions between RcMBL and bacterial and viral pathogens. Importantly, since our RcMBL preparations do not contain the protease zymogen MASP2 (chickens lack MASP 1 and is therefore totally MASP2 driven)(Lynch et al., 2005), we are not able to examine RcMBL-induced complement activation in this study. This requires MASPs or MBL-free serum from chickens.

In conclusion, we successfully expressed a recombinant analogue of MBL from chickens in Hela R19 cell with structural and functional properties similar to that of serum-derived NcMBL. Like NcMBL, RcMBL assembles into higher order oligomers and exhibits Ca^{2+}-dependent sugar binding that is typical for C-type lectins. RcMBL is a fully functional protein as demonstrated by its potential to agglutinate *Salmonella* Typhimurium and to inhibit HA by IAVs. This RcMBL enables to study the role of MBL in non-mammalian species and provides a useful tool for the investigation of its activities against avian pathogens as well as its role in the innate immune system.

Conflict of interest

The authors declare there is no conflict of interest

Acknowledgements

The glycan analysis would not have been possible without the participation of the Protein-Glycan Interaction Resource of the CFG (supporting grant R24 GM098791) and the National Center for Functional Glycomics (NCFG) at Beth Israel Deaconess Medical Center, Harvard Medical School (supporting grant P41 GM103694). Xander de Haan is thanked for his help with the glycan analyses. The work of Onno Bleijerveld and Guanbo Wang was partly supported by the project 'Proteins At Work', financed by the Netherlands Organisation for Scientific Research (NWO) as part of the National Roadmap Large-scale Research Facilities of the Netherlands (project number 184.032.201). Finally, this work was supported by a personal fellowship from the China Scholarship Council (CSC) to Weidong Zhang.

Appendix A. Supplementary data

Supplementary data associated with this article can be found, in the online version, at http://dx.doi.org/10.1016/j.imbio.2016.10.019.

References

Ahn, B.C., Park, J.S., Kim, D., Park, J., Pi, J., Yum, J.S., Jeong, Y., Baek, K., Moon, H.M., Yoon, J., 2013. Overproduction of recombinant human mannose-binding lectin (MBL) in Chinese hamster ovary cells. Protein Expr. Purif. 88, 1–6.

Blixt, O., Head, S., Mondala, T., Scanlan, C., Huflejt, M.E., Alvarez, R., Bryan, M.C., Fazio, F., Calarese, D., Stevens, J., Razi, N., Stevens, D.J., Skehel, J.J., van Die, I., Burton, D.R., Wilson, I.A., Cummings, R., Bovin, N., Wong, C.H., Paulson, J.C., 2004. 2004: Printed covalent glycan array for ligand profiling of diverse glycan binding proteins. Proc. Natl. Acad. Sci. U. S. A. 101, 17033–17038.

Calenge, F., Kaiser, P., Vignal, A., Beaumont, C., 2010. Genetic control of resistance to salmonellosis and to Salmonella carrier-state in fowl: a review. Genet. Sel. Evol. 42 (11-9686-42-11).

Chang, W.C., White, M.R., Moyo, P., McClear, S., Thiel, S., Hartshorn, K.L., Takahashi, K., 2010. Lack of the pattern recognition molecule mannose-binding lectin increases susceptibility to influenza A virus infection. BMC. Immunol. 11 (64-2172-11-64).

Childs, R.A., Feizi, T., Yuen, C.T., Drickamer, K., Quesenberry, M.S., 1990. Differential recognition of core and terminal portions of oligosaccharide ligands by carbohydrate-recognition domains of two mannose-binding proteins. J. Biol. Chem. 265, 20770–20777.

Davies, J.C., Turner, M.W., Klein, N., London MBL CF Study Group, 2004. Impaired pulmonary status in cystic fibrosis adults with two mutated MBL-2 alleles. Eur. Respir. J. 24, 798–804.

Devyatyarova-Johnson, M., Rees, I.H., Robertson, B.D., Turner, M.W., Klein, N.J., Jack, D.L., 2000. The lipopolysaccharide structures of Salmonella enterica serovar Typhimurium and Neisseria gonorrhoeae determine the attachment of human mannose-binding lectin to intact organisms. Infect. Immun. 68, 3894–3899.

Dommett, R.M., Klein, N., Turner, M.W., 2006. Mannose-binding lectin in innate immunity: past, present and future. Tissue Antigens 68, 193–209.

Dyachenko, A., Gruber, R., Shimon, L., Horovitz, A., Sharon, M., 2013. Allosteric mechanisms can be distinguished using structural mass spectrometry. Proc. Natl. Acad. Sci. U. S. A. 110, 7235–7239.

Dyachenko, A., Wang, G., Belov, M., Makarov, A., de Jong, R.N., van den Bremer, E.T., Parren, P.W., Heck, A.J., 2015. Tandem native mass-spectrometry on antibody-drug conjugates and submillion da antibody-antigen protein assemblies on an orbitrap EMR equipped with a high-mass quadrupole mass selector. Anal. Chem. 87, 6095–6102.

Hakansson, K., Reid, K.B., 2000. Collectin structure: a review. Protein Sci. 9, 1607–1617.

Hartshorn, K.L., White, M.R., Shepherd, V., Reid, K., Jensenius, J.C., Crouch, E.C., 1997. Mechanisms of anti-influenza activity of surfactant proteins A and D: comparison with serum collectins. Am. J. Physiol. 273, L1156–66.

Haurum, J.S., Thiel, S., Haagsman, H.P., Laursen, S.B., Larsen, B., Jensenius, J.C., 1993. Studies on the carbohydrate-binding characteristics of human pulmonary surfactant-associated protein A and comparison with two other collectins: mannan-binding protein and conglutinin. Biochem. J. 293 (Pt 3), 873–878.

Heitzeneder, S., Seidel, M., Forster-Waldl, E., Heitger, A., 2012. Mannan-binding lectin deficiency – Good news, bad news, doesn't matter? Clin. Immunol. 143, 22–38.

Hibberd, M.L., Sumiya, M., Summerfield, J.A., Booy, R., Levin, M., 1999. Association of variants of the gene for mannose-binding lectin with susceptibility to meningococcal disease. Meningococcal Res. Group Lancet 353, 1049–1053.

Ikeda, K., Sannoh, T., Kawasaki, N., Kawasaki, T., Yamashina, I., 1987. Serum lectin with known structure activates complement through the classical pathway. J. Biol. Chem. 262, 7451–7454.

Ip, W.K., Takahashi, K., Ezekowitz, R.A., Stuart, L.M., 2009. Mannose-binding lectin and innate immunity. Immunol. Rev. 230, 9–21.

Jensenius, H., Klein, D.C., van Hecke, M., Oosterkamp, T.H., Schmidt, T., Jensenius, J.C., 2009. Mannan-binding lectin: structure, oligomerization, and flexibility studied by atomic force microscopy. J. Mol. Biol. 391, 246–259.

Job, E.R., Deng, Y.M., Tate, M.D., Bottazzi, B., Crouch, E.C., Dean, M.M., Mantovani, A., Brooks, A.G., Reading, P.C., 2010. Pandemic H1N1 influenza A viruses are resistant to the antiviral activities of innate immune proteins of the collectin and pentraxin superfamilies. J. Immunol. 185, 4284–4291.

Juul-Madsen, H.R., Norup, L.R., Handberg, K.J., Jorgensen, P.H., 2007. Mannan-binding lectin (MBL) serum concentration in relation to propagation of infectious bronchitis virus (IBV) in chickens. Viral Immunol. 20, 562–570.

Kawasaki, N., Kawasaki, T., Yamashina, I., 1983. Isolation and characterization of a mannan-binding protein from human serum. J. Biochem. 94, 937–947.

Kjaerup, R.M., Norup, L.R., Skjodt, K., Dalgaard, T.S., Juul-Madsen, H.R., 2013. Chicken mannose-binding lectin (MBL) gene variants with influence on MBL serum concentrations. Immunogenetics 65, 461–471.

Laursen, S.B., Hedemand, J.E., Thiel, S., Willis, A.C., Skriver, E., Madsen, P.S., Jensenius, J.C., 1995. Collectin in a non-mammalian species: isolation and characterization of mannan-binding protein (MBP) from chicken serum. Glycobiology 5, 553–561.

Laursen, S.B., Dalgaard, T.S., Thiel, S., Lim, B.L., Jensen, T.V., Juul-Madsen, H.R., Takahashi, A., Hamana, T., Kawakami, M., Jensenius, J.C., 1998a. Cloning and sequencing of a cDNA encoding chicken mannan-binding lectin (MBL) and comparison with mammalian analogues. Immunology 93, 421–430.

Laursen, S.B., Hedemand, J.E., Nielsen, O.L., Thiel, S., Koch, C., Jensenius, J.C., 1998b. Serum levels, ontogeny and heritability of chicken mannan-binding lectin (MBL). Immunology 94, 587–593.

Ling, M.T., Tu, W., Han, Y., Mao, H., Chong, W.P., Guan, J., Liu, M., Lam, K.T., Law, H.K., Peiris, J.S., Takahashi, K., Lau, Y.L., 2012. Mannose-binding lectin contributes to deleterious inflammatory response in pandemic H1N1 and avian H9N2 infection. J. Infect. Dis. 205, 44–53.

Longo, P.A., Kavran, J.M., Kim, M.S., Leahy, D.J., 2013. Transient mammalian cell transfection with polyethylenimine (PEI). Methods Enzymol. 529, 227–240.

Lu, J.H., Thiel, S., Wiedemann, H., Timpl, R., Reid, K.B., 1990. Binding of the pentamer/hexamer forms of mannan-binding protein to zymosan activates the proenzyme C1r2C1s2 complex, of the classical pathway of complement, without involvement of C1q. J. Immunol. 144, 2287–2294.

Lynch, N.J., Khan, S.U., Stover, C.M., Sandrini, S.M., Marston, D., Presanis, J.S., Schwaeble, W.J., 2005. Composition of the lectin pathway of complement in Gallus gallus: absence of mannan-binding lectin-associated serine protease-1 in birds. J. Immunol. 174, 4998–5006.

Mizuno, Y., Kozutsumi, Y., Kawasaki, T., Yamashina, I., 1981. Isolation and characterization of a mannan-binding protein from rat liver. J. Biol. Chem. 256, 4247–4252.

Neth, O., Jack, D.L., Dodds, A.W., Holzel, H., Klein, N.J., Turner, M.W., 2000. Mannose-binding lectin binds to a range of clinically relevant microorganisms and promotes complement deposition. Infect. Immun. 68, 688–693.

Ng, W.C., Tate, M.D., Brooks, A.G., Reading, P.C., 2012. Soluble host defense lectins in innate immunity to influenza virus. J. Biomed. Biotechnol. 2012, 732191.
Norup, L.R., Dalgaard, T.S., Friggens, N.C., Sorensen, P., Juul-Madsen, H.R., 2009. Influence of chicken serum mannose-binding lectin levels on the immune response towards Escherichia coli. Poult. Sci. 88, 543–553.
Ohl, M.E., Miller, S.I., 2001. Salmonella: a model for bacterial pathogenesis. Annu. Rev. Med. 52, 259–274.
Ohtani, K., Suzuki, Y., Eda, S., Kawai, T., Kase, T., Keshi, H., Sakai, Y., Yamamoto, S., Sakamoto, T., Wakamiya, N., 1999. High-level and effective production of human mannan-binding lectin (MBL) in Chinese hamster ovary (CHO) cells. J. Immunol. Methods 222, 135–144.
Petersen, S.V., Thiel, S., Jensenius, J.C., 2001. The mannan-binding lectin pathway of complement activation: biology and disease association. Mol. Immunol. 38, 133–149.
Reading, P.C., Morey, L.S., Crouch, E.C., Anders, E.M., 1997. Collectin-mediated antiviral host defense of the lung: evidence from influenza virus infection of mice. J. Virol. 71, 8204–8212.
Sheriff, S., Chang, C.Y., Ezekowitz, R.A., 1994. Human mannose-binding protein carbohydrate recognition domain trimerizes through a triple alpha-helical coiled-coil. Nat. Struct. Biol. 1, 789–794.
Shi, L., Takahashi, K., Dundee, J., Shahroor-Karni, S., Thiel, S., Jensenius, J.C., Gad, F., Hamblin, M.R., Sastry, K.N., Ezekowitz, R.A., 2004. Mannose-binding lectin-deficient mice are susceptible to infection with Staphylococcus aureus. J. Exp. Med. 199, 1379–1390.
Thiel, S., Vorup-Jensen, T., Stover, C.M., Schwaeble, W., Laursen, S.B., Poulsen, K., Willis, A.C., Eggleton, P., Hansen, S., Holmskov, U., Reid, K.B., Jensenius, J.C., 1997. A second serine protease associated with mannan-binding lectin that activates complement. Nature 386, 506–510.
Turner, M.W., 1996. Mannose-binding lectin: the pluripotent molecule of the innate immune system. Immunol. Today. 17, 532–540.
Ulrich-Lynge, S.L., Dalgaard, T.S., Norup, L.R., Song, X., Sorensen, P., Juul-Madsen, H.R., 2015. Chicken mannose-binding lectin function in relation to antibacterial activity towards Salmonella enterica. Immunobiology 220, 555–563.
Veldhuizen, E.J., van Eijk, M., Haagsman, H.P., 2011. The carbohydrate recognition domain of collectins. FEBS J. 278, 3930–3941.
Vorup-Jensen, T., Sorensen, E.S., Jensen, U.B., Schwaeble, W., Kawasaki, T., Ma, Y., Uemura, K., Wakamiya, N., Suzuki, Y., Jensen, T.G., Takahashi, K., Ezekowitz, R.A., Thiel, S., Jensenius, J.C., 2001. Recombinant expression of human mannan-binding lectin. Int. Immunopharmacol. 1, 677–687.
Wang, G., Johnson, A.J., Kaltashov, I.A., 2012. Evaluation of electrospray ionization mass spectrometry as a tool for characterization of small soluble protein aggregates. Anal. Chem. 84, 1718–1724.
Weis, W.I., Kahn, R., Fourme, R., Drickamer, K., Hendrickson, W.A., 1991. Structure of the calcium-dependent lectin domain from a rat mannose-binding protein determined by MAD phasing. Science 254, 1608–1615.
Weis, W.I., Drickamer, K., Hendrickson, W.A., 1992. Structure of a C-type mannose-binding protein complexed with an oligosaccharide. Nature 360, 127–134.
Yang, J., Yan, R., Roy, A., Xu, D., Poisson, J., Zhang, Y., 2015. The I-TASSER Suite: protein structure and function prediction. Nat. Methods 12, 7–8.
de Vries, R.P., de Vries, E., Bosch, B.J., de Groot, R.J., Rottier, P.J., de Haan, C.A., 2010. The influenza A virus hemagglutinin glycosylation state affects receptor-binding specificity. Virology 403, 17–25.
van Eijk, M., van de Lest, C.H., Batenburg, J.J., Vaandrager, A.B., Meschi, J., Hartshorn, K.L., van Golde, L.M., Haagsman, H.P., 2002. Porcine surfactant protein D is N-glycosylated in its carbohydrate recognition domain and is assembled into differently charged oligomers. Am. J. Respir. Cell Mol. Biol. 26, 739–747.
van Eijk, M., Bruinsma, L., Hartshorn, K.L., White, M.R., Rynkiewicz, M.J., Seaton, B.A., Hemrika, W., Romijn, R.A., van Balkom, B.W., Haagsman, H.P., 2011. Introduction of N-linked glycans in the lectin domain of surfactant protein D: impact on interactions with influenza A viruses. J. Biol. Chem. 286, 20137–20151.
van den Heuvel, R.H., van Duijn, E., Mazon, H., Synowsky, S.A., Lorenzen, K., Versluis, C., Brouns, S.J., Langridge, D., van der Oost, J., Hoyes, J., Heck, A.J., 2006. Improving the performance of a quadrupole time-of-flight instrument for macromolecular mass spectrometry. Anal. Chem. 78, 7473–7483.